CHIN. PHYS. LETT. Vol. 36, No. 4 (2019) 048201

Double Resonance Raman Scattering in Single-Layer $MoSe_2$ under Moderate Pressure *

Jian-mei Li(李健梅)[1,2], Yi-kun Yao(姚一锟)[1,2], Li-huan Sun(孙丽欢)[1,2], Xin-yan Shan(单欣岩)[1], Cong Wang(王聪)[5], Xing-hua Lu(陆兴华)[1,2,3,4]**

[1]*Beijing National Laboratory for Condensed Matter Physics, Institute of Physics, Chinese Academy of Sciences, Beijing 100190*
[2]*School of Physical Sciences, University of Chinese Academy of Sciences, Beijing 100190*
[3]*Center for Excellence in Topological Quantum Computation, Beijing 100190*
[4]*Songshan Lake Materials Laboratory, Dongguan 523808*
[5]*School of Physics & Mathematical Sciences, Nanyang Technological University, Singapore 639798, Singapore*

(Received 4 December 2018)

Pressure-dependent properties in layered transition-dichalcogenides are important for our understanding of their basic structures and applications. We investigate the electronic structure in $MoSe_2$ monolayer under external pressure up to 5.73 GPa by Raman spectroscopy and photoluminescence (PL) spectroscopy. The double resonance out-of-plane acoustic mode ($2ZA$) phonon is observed in Raman spectroscopy near 250 cm^{-1}, which presents pronounced intensity and pressure dependence. Significant variation in $2ZA$ peak intensity under different pressures reflects the change in electronic band structure as pressure varies, which is consistent with the blue shift in PL spectroscopy. The high sensitivity in both Raman and PL spectroscopy under moderate pressure in such a two-dimensional material may have many advantages for optoelectronic applications.

PACS: 82.80.Gk, 81.40.Vw DOI: 10.1088/0256-307X/36/4/048201

Transition metal dichalcogenides (TMDs) MX_2 (e.g., M=Mo or W, X=S, Se or Te) are layered structures similar to graphite. Generally, MX_2 shows an indirect to direct gap evolution as the material changes from bulk to monolayer,[1,2] offering an interesting platform to explore two-dimensional (2D) excitons, phonons, and the interplay between spin and valley electrons.[3–5] In contrast to gapless graphene, the finite band gap of 1–2 eV in MX_2, and its flexibility and transparency are highly attractive for construction of transistors[6,7] and photodetectors[8,9] for novel electronic and optoelectronic applications. Significant progress has been made in tuning the properties of TMDs, mainly by varying the thickness,[10] applying strain,[11] or electrostatic doping.[12]

Considering their possible applications in flexible electronic devices, the pressure effect on 2D materials are of particular value to fully understand the underlying physics including photonic, mechanical and electronic properties.[13,14] So far, most pressure-dependent studies in TMD materials have been focused on MoS_2. It has been demonstrated that the band structure of monolayer MoS_2 can be tuned through pressure engineering. A $2H_c$ to $2H_a$ iso-structural phase transition has been observed in bulk MoS_2 as a result of layer sliding under a pressure above 20 GPa and the material becomes metallic around 4 GPa,[15] in agreement with theoretical predictions.[16] Similarly, a semiconductor to metal transition in multilayer MoS_2 has also been observed by applying pressure around 19 GPa.[17] $MoSe_2$ is similar to iso-structural MoS_2 possessing similar electronic structures. Since the Se^{2-} has broader electron orbitals than S^{2-}, $MoSe_2$ has stronger interlayer interactions. In addition, $MoSe_2$ undergoes a semiconductor-to-metal transition without structural transition,[13,18–20] possessing a different pressure-dependent behavior as compared to MoS_2. It is thus attractive for applications based on materials with tunable optical and electronic properties. Although the physical properties in layered $MoSe_2$ such as their crystal structures,[21,22] stacking orders,[23–25] lattice vibration modes, and interlayer couplings[22,26] have been extensively explored by Raman spectroscopy, reports on pressure-dependent characterization of monolayer $MoSe_2$ have been very limited.

In this work, we performed Raman spectroscopy and photoluminescence (PL) spectroscopy on monolayer $MoSe_2$ under elevated pressures up to 5.73 GPa. Even under such moderate pressure, the Raman spectra present clear signature of the double resonance out-of-plane acoustic ($2ZA$) mode and a remarkable change as pressure varies. The observation suggests very high quality of the monolayer sample and illustrates changes in the electronic band structure and in the resonant excitation process. The pressure-dependent PL spectra provide additional evidence for our explanation.

Figure 1(a) shows the atomic model structure in both in-plane and out-of-plane directions for $MoSe_2$. Mo and Se represent the molybdenum and Selenium atoms, respectively. The single layer $MoSe_2$ is actually a 'three-layer' structure consisting of a Mo layer sandwiched between two Se layers. The $MoSe_2$ sample

*Supported by the Strategic Priority Research Program (B) of the Chinese Academy of Sciences under Grant Nos XDB30000000, XDB28000000 and XDB07030100, the National Natural Science Foundation of China under Grant Nos 11774395, 11727902 and 91753136, and the Beijing Natural Science Foundation under Grant No 4181003.
**Corresponding author. Email: xhlu@aphy.iphy.ac.cn
© 2019 Chinese Physical Society and IOP Publishing Ltd

in our experiment was grown by chemical vapor deposition (CVD) on the c-plane sapphire crystal surface. Figure 1(b) shows the typical as-grown 2D monolayer structures imaged by an optical microscope, where edges of these structures range from 5 to 30 μm in length. The samples have clear geometrical symmetry and optical contrast, indicating their monolayer nature.

The pressure-dependent Raman and PL measurements were performed using a diamond anvil cell (DAC) device, with two diamond culets with 400 μm in diameter, as shown in Fig. 1(c). Because the horizontal dimension of the sample was larger than the DAC gasket chamber, diamond is pressed directly onto the sample without pressure transmitting medium.[27,28] To explore the phenomenon of the maximum pressure range in our experiment, we applied pressure to the sample until the substrate broke down, typically around 6 GPa. The spectra were collected using a Renishaw inVia micro Raman system with a 488 nm laser excitation. The laser power density is limited below 0.64 mW/ μm^2 in order not to cause any damage in the sample or shift in Raman modes due to the heating effect. The Raman and PL spectra were collected simultaneously on the same spot. Since the laser spot size was about 1 μm, the pressure over the measurement area could be regarded homogenous. The pressure was increased by tightening external screws, and the pressure was gauged using the sapphire pressure calibrator method,[29] and the relationship between pressure and the 417 cm^{-1} Raman peak shift can be expressed as

$$P = 252.021 \cdot \Delta\omega(417\,\mathrm{cm}^{-1}) + 87.2192 \cdot \Delta\omega(417\,\mathrm{cm}^{-1})^2\,(\mathrm{MPa}). \quad (1)$$

The pressure-dependence measurements were taken at room temperature with pressure increasing up to 5.73 GPa.

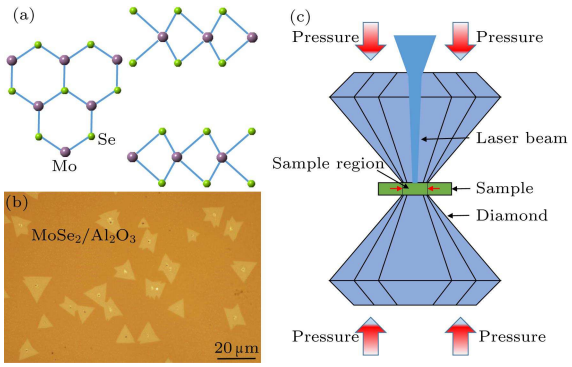

Fig. 1. (a) Schematic diagrams of the lattice structure of $MoSe_2$ in both in-plane (left) and out-of-plane (right) directions. Se atoms are shown as green spheres while Mo atoms are presented by purple spheres. (b) An optical micrograph of monolayer $MoSe_2$ (scale bar: 20 μm). (c) A schematic drawing of the diamond anvil cell (DAC), and the pressure is applied on the sample by tightening external screws.

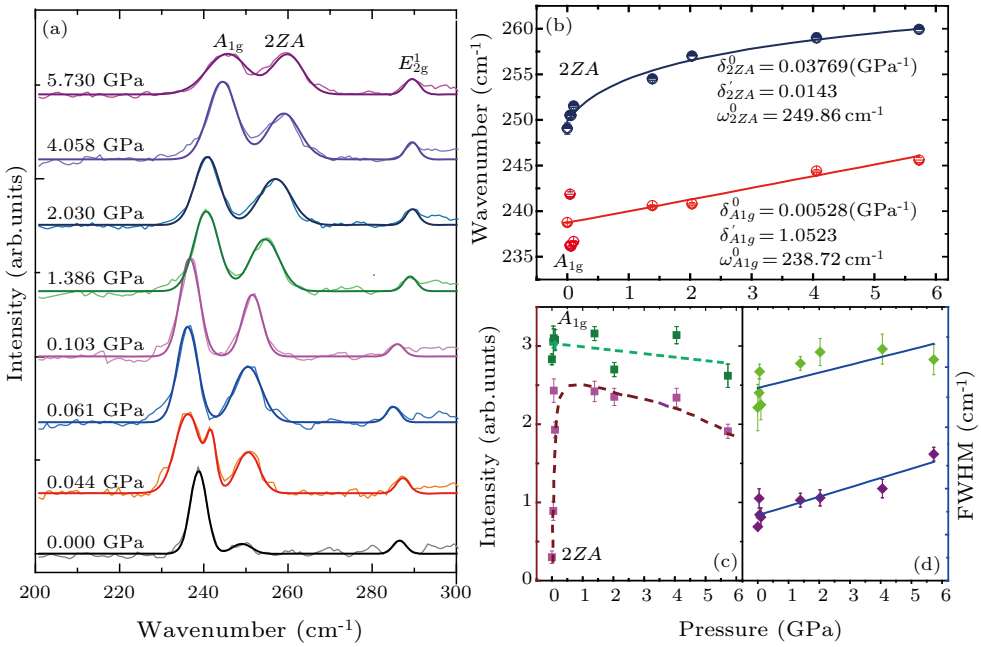

Fig. 2. (a) Raman spectra of the monolayer $MoSe_2$ sample onto a c-plane sapphire substrate measured under various pressures and at ambient temperature excited by 488 nm laser. The curves can be fitted using multi-peaks Gaussian function. The data have been normalized to the intensity of the c-plane sapphire substrate around 417 cm^{-1} peak, and the curves are shifted vertically to improve visual clarity. (b) The Raman wavenumber of A_{1g} and $2ZA$ modes as a function of external pressure. The A_{1g} and $2ZA$ modes are represented by red and blue solid circles, respectively. (c) Evolution of the peaks intensity for both A_{1g} and $2ZA$ modes, and the dashed line is drawn as guide to the eyes. (d) The FWHM of both A_{1g} and $2ZA$ modes as a function of external pressure.

Figure 2(a) displays the Raman spectra of a monolayer $MoSe_2$ at room temperature under different pressures. Characteristic Raman peaks include a sharp one at 239 cm^{-1} as assigned to A_{1g} mode, and a broad one at higher wavenumber 286 cm^{-1} as of E^1_{2g} mode. In general, the characteristics of both modes

agree well with the previous results of exfoliated 2H-phase $MoSe_2$ and CVD-grown $MoSe_2$ films.[27–35] We are particularly interested in the observation of double resonance out-of-plane acoustic ($2ZA$) mode at 250 cm^{-1}. The $2ZA$ mode is a second-order Raman mode resulted from a double resonance (DR) process involving the acoustic mode (ZA) around 125 cm^{-1}. It is intrinsic to the monolayer $MoSe_2$ only and it can be used to judge the quality of the sample.[36] The clear $2ZA$ mode further confirms the high quality of the monolayer $MoSe_2$ sample.

Abnormal features under relatively low pressure have been noticed. The A_{1g} mode splits into two peaks under a very gentle pressure of 0.04 GPa. Upon further increasing pressure, the higher one disappears and the lower one shifts toward higher wavenumber. The intensity of $2ZA$ mode increases abruptly as pressure increases up to 0.1 GPa. Considering the fact that the pressure was applied without transmission medium, the abnormal features at low pressure are likely to be due to the anisotropic strain during the initial contact of diamond culet with the sample. At higher pressure, the sample endures uniaxial strain and the substrate effect can be neglected. We ignore these abnormal features in this study.

The pressure-dependent energy shift in the linear region, from 0.1 to 5.73 GPa can be fitted using the function[37,38]

$$\omega_i(P)/\omega_i^0 = [(\delta_i^0/\delta_i') \times P + 1]^{\delta_i'}, \quad (2)$$

where δ_i' is taken as the free fitting parameters, ω_i^0 represents frequency of the ith mode under zero external pressure, and δ_i^0 is its logarithmic pressure coefficient ($(d\ln\omega_i/dP)_{P=0}$). For the A_{1g} mode, we set $\delta_i' = 1$ for a simple linear fit and derive the value of pressure coefficient as 1.71 cm^{-1}/GPa, which is consistent with previous studies.[27,38] We also extracted the intensity and the full width at half maximum (FWHM) for both A_{1g} and 2 ZA modes, using the multi-peak Gaussian function fitting, as shown in Figs. 2(c) and 2(d). For both of the modes, the FWHM as a function of pressure shows linear increase up to 5.73 GPa, indicating no phase transition within the pressure range in our experiment.[17,37]

We measured the PL peak as a function of pressure in the meantime. To obtain the energy of the PL peak, the PL spectra are fitted by the Lorenz function as shown Fig. 3(a). Except for the initial-contact points, the peak shifts toward higher energy as pressure continually increases. The blue shift of PL peak can be fitted with a second-order polynomial[39]

$$E_g = E_{P=0} + aP + bP^2, \quad (3)$$

where $E_{P=0}$ is the initial energy of PL peak at room temperature, a is dE/dP, and b is d^2E/dP^2. The fitting result agrees with the theoretical calculation for the upward shift of the K valley of the conduction band under uniaxial strain.[39,40] The decrease in intensity of PL as pressure increases exhibits a common observation in a similar pressure-dependent experiment. These phenomena may happen because of the strain-induced direct-to-indirect transition,[39] the pressure-induced increase of defects,[41] or a pressure-driven decrease in oscillator strength.[42] However, more experimental studies are required to clarify this point.

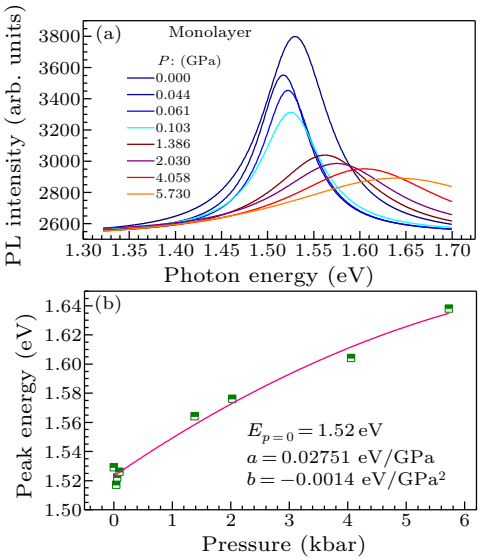

Fig. 3. (a) Photoluminescence spectra under external pressure from 0 to 5.73 GPa. (b) The energy of PL peak as a function of pressure, fitted by a second order polynomial function.[39]

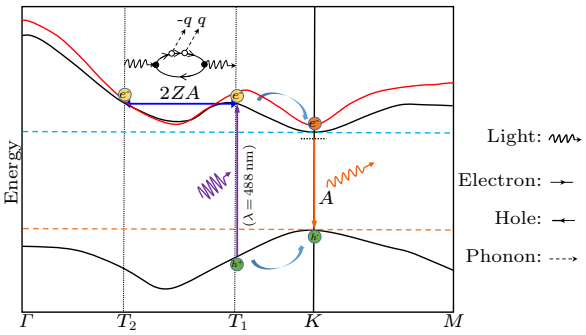

Fig. 4. Schematic representations of the electronic band structure for monolayer $MoSe_2$ at $P = 0$ GPa (black line) and $P \sim 5$ GPa (red line), respectively. The two dashed lines (orange and light blue) illustrate the edges of related electronic bands. Some of electrons excited by the 488-nm laser move to bottom of the conduction band at K point, while holes relax to top of the valence band, creating A exciton before recombination. Meanwhile, electrons at T_1 and T_2 can be scattered by the ZA phonons. The two-phonon process is shown in the inset.

We infer the schematic diagram of the evolution of the band structure under pressure for monolayer $MoSe_2$ referring to the calculated band structure (without spin orbit coupling).[40] By absorbing the 488-nm photon, electrons in the valence band are excited to the conduction band. Following energy consideration, the excited electrons locate close to the local maximum of the conduction band, as shown in Fig. 4. The excited electrons can be further scattered by the ZA phonon at T_1 and T_2, producing the double resonance effect. The whole Raman scattering process is illustrated as the inset of Fig. 4. First, the electron

is excited into the conductive band with a certain momentum. Second, the excited electron is scattered into another state by emitting a phonon with momentum $-q$. In the third step, the electron is scattered back to initial excited state, by emitting the phonon with momentum q. Finally, the electron and hole recombine vertically, emitting the light.[43,44] We note that such a process can be observed only in pure crystalline samples.

The $2ZA$ Raman intensity can be formulated from golden rule generalized to the fourth order,[36,43,45]

$$I \propto \sum_{f} \sum_{\mathrm{a,b,c}} \left| (M_{\mathrm{fc}} M_{\mathrm{cb}} M_{\mathrm{ba}} M_{\mathrm{ai}}) / \left[\left(\varepsilon_{\mathrm{i}} - \varepsilon_{\mathrm{c}} - i\frac{\gamma^{\mathrm{c}}}{2} \right) \cdot \left(\varepsilon_{\mathrm{i}} - \varepsilon_{\mathrm{b}} - i\frac{\gamma^{\mathrm{b}}}{2} \right) \left(\varepsilon_{\mathrm{i}} - \varepsilon_{\mathrm{a}} - i\frac{\gamma^{\mathrm{a}}}{2} \right) \right] \right|^2 \times \delta(\varepsilon_{\mathrm{i}} - \varepsilon_{\mathrm{f}}), \tag{4}$$

where ε_{i} is the energy of the laser, ε_{a}, ε_{b} and ε_{c} are energies of excited states (electrons and phonons), ε_{f} is the energy of the final state, γ^{a}, γ^{b} and γ^{c} are the inverse of the lifetimes of the excited electronic virtual states a, b and c, and δ is the delta function. The process M_{ai} corresponds to the absorption of light by creating an electron-hole pair. The electron-phonon coupling matrices M_{ba} and M_{cb} indicate that the carriers are scattered twice by ZA phonon before recombination. Finally, the process M_{fc} corresponds to the recombination of carriers by light emission. If we assume that the matrices M are constant, the Raman intensity is then determined by the denominator and the density of states. The denominator is proportional to the square of the energy of $2ZA$ mode, $(\hbar\omega_{\mathrm{p}})^2$. Simple calculation derives a contribution of 8% in changes of Raman intensity as pressure increases up to 5.73 GPa. In contrast, our experiment shows a 20% change in intensity of the Raman $2ZA$ mode under this pressure variation. The other contribution is due to the changes in density of states. As pressure increases, the conductive band moves up to a higher energy. This results in a decreased density of states as T_1 contour shifts away from the local maximum of the conduction band.

In summary, we have studied the photoluminescence and Raman spectroscopy in a high-quality monolayer $MoSe_2$ sample under moderate pressures. The quality of the sample is ensured by clear Raman signal of double resonant $2ZA$ mode. Except for the initial contact under very low pressure, the $2ZA$ phonon energy shifts to higher wavenumber and the Raman peak intensity decreases monotonously as the external pressure increases up to 5.73 GPa. The observations have been explained by the electron-phonon interaction and the changes in electronic band structure under pressure. Sensitive Raman and PL spectroscopy in such a 2D material under moderate pressures is attractive for a large number of applications, such as sensors and optoelectronics.

References

[1] Splendiani A et al 2010 *Nano Lett.* **10** 1271
[2] Mak K F et al 2010 *Phys. Rev. Lett.* **105** 136805
[3] Zhou Y et al 2017 *Nat. Nanotechnol.* **12** 856
[4] Xu X et al 2014 *Nat. Phys.* **10** 343
[5] Plechinger G et al 2016 *Nat. Commun.* **7** 12715
[6] Cui X et al 2015 *Nat. Nanotechnol.* **10** 534
[7] Li X X et al 2017 *Nat. Commun.* **8** 970
[8] Claassen M et al 2016 *Nat. Commun.* **7** 13074
[9] Mak K F and Shan J 2016 *Nat. Photon.* **10** 216
[10] Soubelet P et al 2016 *Phys. Rev. B* **93** 155407
[11] Lee J U et al 2017 *Nat. Commun.* **8** 1370
[12] Wang Y et al 2017 *Nature* **550** 487
[13] Zhao Z et al 2015 *Nat. Commun.* **6** 7312
[14] Nayak A P et al 2015 *Nano Lett.* **15** 346
[15] Chi Z H et al 2014 *Phys. Rev. Lett.* **113** 036802
[16] Hromadová L et al 2013 *Phys. Rev. B* **87** 144105
[17] Nayak A P et al 2014 *Nat. Commun.* **5** 3731
[18] Kohulák O and Martoňák R 2017 *Phys. Rev. B* **95** 054105
[19] Rifliková M et al 2014 *Phys. Rev. B* **90** 035108
[20] Dybala F et al 2016 *Sci. Rep.* **6** 26663
[21] Lee C, Yan H, Brus L E, Heinz T F, Hone J and Ryu S 2010 *ACS Nano* **4** 2695
[22] Zhang X et al 2015 *Chem. Soc. Rev.* **44** 2757
[23] Puretzky A A et al 2015 *ACS Nano* **9** 6333
[24] Cong C et al 2011 *ACS Nano* **5** 8760
[25] Zhang X et al 2016 *Carbon* **99** 118
[26] Zhang X et al 2016 *Nanoscale* **8** 6435
[27] Gao R and Li H 2012 *High Press. Res.* **32** 176
[28] Yang M et al 2017 *Appl. Phys. Lett.* **110** 093108
[29] Roy A, Movva H C, Satpati B, Kim K, Dey R, Rai A, Pramanik T, Guchhait S, Tutuc E and Banerjee S K 2016 *ACS Appl. Mater. Interfaces* **8** 7396
[30] Chen J, Zhao X, Tan S J, Xu H, Wu B, Liu B, Fu D, Fu W, Geng D, Liu Y, Liu W, Tang W, Li L, Zhou W, Sum T C and Loh K P 2017 *J. Am. Chem. Soc.* **139** 1073
[31] Wang X, Gong Y, Shi G, Chow W L, Keyshar K, Ye G, Vajtai R, Lou J, Liu Z, Ringe E, Tay B K and Ajayan P M 2014 *ACS Nano* **8** 5125
[32] Chang Y H, Zhang W, Yihan Zhu, Yu Han, Pu J, Chang J K, Hsu W T, Huang J K, Hsu C L, Chiu M H, Takenobu T, Li H, Wu C I, Chang W H, Wee A T S and Li L J 2014 *ACS Nano* **8** 8582
[33] Lu X, Utama M I, Lin J, Gong X, Zhang J, Zhao Y, Pantelides S T, Wang J, Dong Z, Liu Z, Zhou W and Xiong Q 2014 *Nano Lett.* **14** 2419
[34] Zhao Y, Lee H, Choi W, Fei W and Lee C J 2017 *RSC Adv.* **7** 27969
[35] Nam D, Lee J U and Cheong H 2015 *Sci. Rep.* **5** 17113
[36] Bilgin I, Raeliarijaona A S, Lucking M C, Hodge S C, Mohite A D, de Luna Bugallo A, Terrones H and Kar S 2018 *ACS Nano* **12** 740
[37] Postorino P, Congeduti A, Degiorgi E, Itié J P and Munsch P 2002 *Phys. Rev. B* **65** 224102
[38] Caramazza S, Capitani F, Marini C, Mancini A, Malavasi L, Dore P and Postorino P 2017 *J. Phys.: Conf. Ser.* **950** 042012
[39] Fu X, Li F, Lin J F, Gong Y, Huang X, Huang Y, Han B, Zhou Q and Cui T 2017 *J. Phys. Chem. Lett.* **8** 3556
[40] Chang C H, Fan X, Lin S H and Kuo J L 2013 *Phys. Rev. B* **88** 195420
[41] Xiuming Dou, Kun Ding, Desheng Jiang and Sun B 2014 *ACS Nano* **8** 7458
[42] Xiao G, Cao Y, Qi G, Wang L, Liu C, Ma Z, Yang X, Sui Y, Zheng W and Zou B 2017 *J. Am. Chem. Soc.* **139** 10087
[43] Venezuela P, Lazzeri M and Mauri F 2011 *Phys. Rev. B* **84** 035433
[44] Thomsen C and Reich S 2000 *Phys. Rev. Lett.* **85** 5214
[45] Martin R M and Falicov L M 1983 *Top. Appl. Phys.* **8** 79